Food Bioscience 41 (2021) 100986

Contents lists available at ScienceDirect

Food Bioscience

journal homepage: www.elsevier.com/locate/fbio

Decellularized spinach: An edible scaffold for laboratory-grown meat

Jordan D. Jones [a], Alex S. Rebello [a], Glenn R. Gaudette [b,*]

[a] Biomedical Engineering, Worcester Polytechnic Institute, Worcester, MA, 01609, USA
[b] Department of Engineering, Boston College, Chestnut Hill, MA, 02436, USA

ARTICLE INFO

Keywords:
Laboratory-grown meat
Cellular agriculture
In vitro meat production
Cultured meat

ABSTRACT

It is projected that by the year 2050, there will be insufficient land suitable for agriculture to feed the world. Cellular agriculture has the potential to produce meat that replicates the structure of traditionally produced meat while minimizing the land needed. There is a need for an edible scaffold suitable for the growth of animal muscle. This study showed that decellularizing spinach leaves produced an edible scaffold that has a vascular network that could potentially maintain the viability of primary bovine satellite cells as they develop into meat. Primary bovine satellite cells were cultured on the surface of decellularized spinach leaves and gelatin coated glass for 7 and 14 days. After 14 days, primary bovine satellite cells seeded on the decellularized leaf scaffold maintained ~99% viability; and ~25% of the cells showed expression of myosin heavy-chain. Cell alignment varied between animals from which the cells were acquired. Areas of alignment were observed showing an average kappa value for cytoskeletal alignment of 0.71 ± 0.1 after 14 days in culture. There was no statistical significance in each category between cells cultured on gelatin coated glass and decellularized spinach leaves. These results suggested that decellularized spinach is a cost-efficient and environmentally friendly scaffold, that can potentially accelerate the development of laboratory-grown meat by providing an edible substrate for bovine satellite cells.

1. Introduction

The future of Earth depends on the exploration of methods to reduce activities that result in destructive environmental changes. Developing a sustainable method of meat production is becoming a challenge facing modern society. The land allocated for the cultivation of grazing livestock is equivalent to 26% of Earth's ice-free land (Ellis et al., 2010). Future projections show that a growing population and demand for meat poses a risk of insufficient land to feed the world by the year 2050 using current methods of livestock cultivation (Aiking, 2011; Ray et al., 2013). The need for land to raise livestock has resulted in deforestation around the world, causing damage to the Amazon rainforest and threatening much of its endemic wildlife (Hasan et al., 2019). Advocates for eliminating meat from American diets have stressed the need for dietary reformation, yet only 5% of Americans are vegetarian (Shapiro, 2018).

Tissue engineering techniques can be used to create meat *in vitro* by expanding cells acquired from small samples of muscle tissue. This process may eliminate some of the need for large livestock herds and has the potential to reduce greenhouse gas emissions and land requirements (Burton et al., 2000). Meeting this need would require replicating the structure of traditional meat. Producing structured meat, like steaks, presents challenges in oxygen diffusion (Novosel et al., 2011). Due to the limitations of oxygen diffusion, a cell must be within 200 μm of a nutrient source to remain viable (Novosel et al., 2011). *In vivo*, thick tissues have a complex network of vasculature that provides cells with constant access to oxygen and nutrients. There is currently no definitive tissue engineered solution for vascularized 3D cultures *in vitro*. Previous studies have shown that decellularized spinach leaves can serve as a vascularized scaffold which supports various mammalian cell types (Fontana et al., 2017; Gershlak et al., 2017). In addition to its vasculature, decellularized spinach has many characteristics that make it an ideal biomaterial for developing meat. Spinach leaves are cost-efficient, environmentally friendly, edible, and void of animal-derived components found in other common biomaterial scaffolds such as gelatin. This study expands upon the results of previous studies to evaluate the efficacy of decellularized spinach in laboratory-grown meat applications by evaluating viability, differentiation potential, and local alignment of seeded bovine primary satellite cells.

* Corresponding author. Boston College Department of Engineering, 140 Commonwealth Ave, Chestnut Hill, MA, 02436, USA.
E-mail address: gaudettg@bc.edu (G.R. Gaudette).

https://doi.org/10.1016/j.fbio.2021.100986
Received 17 March 2020; Received in revised form 7 March 2021; Accepted 9 March 2021
Available online 20 March 2021

2. Materials and methods

2.1. Experiment design

The following experiments measured viability, differentiation, and alignment. Each experiment was done with three biological replicates with cells isolated from three different live cows (2-yr-old male Holsteins raised for meat without growth stimulants) grown on decellularized spinach. These biological replicates were referred to as cow 1, cow 2, and cow 3. The three animals used were all sourced from a local slaughter facility (Adams Farm, Athol, MA, USA) and slaughtered using electrical stunning. Tissue samples were collected from the shank area of the front legs. Each biological replicate had three technical replicates for a total sample size of 9. Studies have shown that collagen, in the form of gelatin, shows promise for cell growing food applications (Datar & Betti, 2010). Therefore, cells grown on decellularized spinach were compared to a control group of isolated satellite cells grown on glass slides coated with gelatin. Each experiment was completed at two time points: 7 and 14 days. At the end of each time point, the samples were fixed in 4% paraformaldehyde for 10 min.

2.1.1. Imaging and analysis

Unless specified otherwise, samples were imaged using a Leica SP5 point scanning confocal microscope (Leica Microsystems, Wetzlar, Germany) at 20X. Five images were taken in total. One image was taken from the center of the scaffold and from 4 locations around the edges of the seeded area.

2.1.2. Statistical analysis

All statistical analysis was done using GraphPad Prism 9.0.0_121 (Graphpad, San Diego, CA, USA). Unless specified otherwise, all the data is expressed as mean ± standard deviation. All comparisons were made with either an ordinary one-way ANOVA or Welch's *t*-test. A p value of <0.05 was used as the threshold of statistical significance.

2.2. Spinach leaf decellularization and scaffold preparation

The immersion method of plant decellularization (Fontana et al., 2017) was used in lieu of the original perfusion method of plant decellularization (Gershlak et al., 2017). This is because the perfusion method requires that each leaf be cannulated individually, a time intensive process.

Triple washed packaged baby spinach leaves (Olivia's Organics, Chelsea, MA, USA) were acquired from a local food store. Spinach cuticles were removed by agitating the leaves in 98% hexane (VWR, Radnor, PA, USA) for 3 min followed by 1x phosphate buffered saline (PBS) (137 mM NaCl, 112.7 mM KCl, 10 mM Na_2HPO_4, 1.8 mM KH_2PO_4in deionized water) for 3 min. The deionized water used in all solutions was generated using the Ultrapure Direct-Q water system (MilliporeSigma, Burlington, MA, USA). Cuticle removal was achieved after three cycles of hexanes and PBS treatment. After complete cuticle removal, spinach leaves were placed in 50 ml conical tubes and submerged in 1% sodium dodecyl sulfate (SDS) (Sigma-Aldrich, St. Louis, MO, USA) in deionized water for 5 days, refreshing the solution every 24 hr. After the initial 5 days, the SDS solution was replaced with 0.1% Triton X-100 (Sigma-Aldrich) and 10% concentrated bleach (The Clorox Co., Oakland, CA, USA) in deionized water for 48 hr, refreshing the solution after 24 hr. The spinach leaves were then rinsed in deionized water for 24 hr. After rinsing, the leaves were placed in 10 mM tris buffer (Sigma-Aldrich) for 24 hr. The leaves were stored at −20°C overnight. Lyophilization (FreeZone Triad 74000 series, Labconco Corp., Kansas City, MO, USA) was done at −25°C and 0.210 Torr over 24 hr. Decellularized spinach scaffolds were stored at room temperature until needed for a maximum of two wk. The ambient temperature in the room was not monitored.

2.2.1. DNA analysis of decellularized leaf scaffolds

Samples were first prepared by taking 12.7 mm diameter circular biopsy punches from each lyophilized decellularized leaf. DNA content was quantified to confirm complete decellularization. Samples were then cut (1 x 1 mm) and added to a 1.5 ml microcentrifuge tube (Eppendorf, Hamburg, Germany). Samples were flash-frozen in liquid nitrogen and immediately pulverized using a mortar and pestle to further reduce the size of the samples. The DNA content of the samples was measured using a CYQUANT® DNA assay kit (Thermo Fisher Scientific, Waltham, MA, USA), a fluorescence-based DNA quantification method. To release the DNA present in the sample, the pulverized samples were each combined with 100 μl of the lysis buffer included in the CYQUANT® DNA assay kit. The released DNA was then fluorescently labeled by adding 100 μl of the CYQUANT® GR dye. Decellularized leaf samples were compared to a standard curve created by serial dilution of a DNA standard and non-decellularized leaf samples as a control. Fluorescence intensity was measured using a PerkinElmer Victor3 spectrophotometer (PerkinElmer, Waltham, MA, USA) with an excitation wavelength of 480 nm and a emission wavelength of 530 nm. The fluorescence intensity value is then converted to DNA content through a linear regression of the standard curve values.

2.3. Primary satellite cell isolation and culture conditions

2.3.1. Primary satellite cell isolation

The muscle samples were kept in separate containers on ice for 30 min during transportation from the slaughter facility to the laboratory. Satellite cell isolation began immediately upon arrival (Fig. 1). The entire isolation was completed inside a laminar flow hood. All instruments and dishes were sterilized in a Tuttnauer EZ9-PLUS Steam Sterilizer (Tuttnauer NY, Huappauge, NY, USA) prior to isolation. The muscle tissue was placed onto a sterile dish and soaked in rinse medium (Ham's Dulbecco's modified Eagle's medium (DMEM/F12) (Thermo Fisher Scientific), 1% each of penicillin/streptomycin (P/S) (Thermo Fisher Scientific) for 10 min.

Exposure of inner tissue was done by making a shallow horizontal cut through the center of the muscle. The muscle tissue on either side of this cut was excised away with a set of sterile tools to complete further exposure of the interior tissue. Samples were taken from the exposed interior muscle and dissected into ~1 mm^3 pieces. The samples were then placed in a sterile dish containing digestion medium (Ham's DMEM/F12, 1% P/S, 10% recombinant collagenase sourced from *Clostridium histolyticum* (Worthington, Lakewood, NJ, USA) and incubated at 37°C for 1 hr, periodically swirling the dish every 15 min. The content of the dish was transferred to a 50 ml conical tube and allowed to settle to the bottom. The supernatant was removed and filtered using a 100 μm sterile cell strainer (VWR) into a 50 ml conical tube and centrifuged at 300×*g* at room temperature for 5 min. The tissue pellet was resuspended in 25 ml of sterile rinse medium (Ham's DMEM/F12, 1% P/S). Filtration was completed using three 70 μm and three 40 μm cell strainers (Thermo Fisher Scientific), centrifuging as stated above, and resuspending the pellet after each filtration. After the final filtration, the pellet was resuspended in 12 ml of growth medium (Ham's DMEM/F12, 10% heat-inactivated fetal bovine serum (FBS) Thermo Fisher Scientific, 1% P/S, 4 ng/ml recombinant human fibroblast growth factor – 2 (FGF2), 2.5 ng/ml recombinant human hepatocyte growth factor (HGF), 10 ng/ml recombinant human epidermal growth factor (EGF), and 5 ng/ml recombinant human insulin-like growth factor – 1 (IGF)). The isolated cells were incubated overnight at 37°C and 5% CO_2 with a HERAcell 150i CO_2 incubator (Thermo Fisher Scientific) to allow cell attachment.

Due to the inherent heterogeneity of the isolated population, it was necessary to enrich the population of satellite cells. Previous studies have shown that the satellite cell population can be enriched using differential adhesion pre-plating (Eberli et al., 2009). This was done by plating the cell suspension on non-tissue culture polystyrene Petri dishes (Thermo Fisher Scientific) and incubating at 37°C and 5% CO_2 for 30

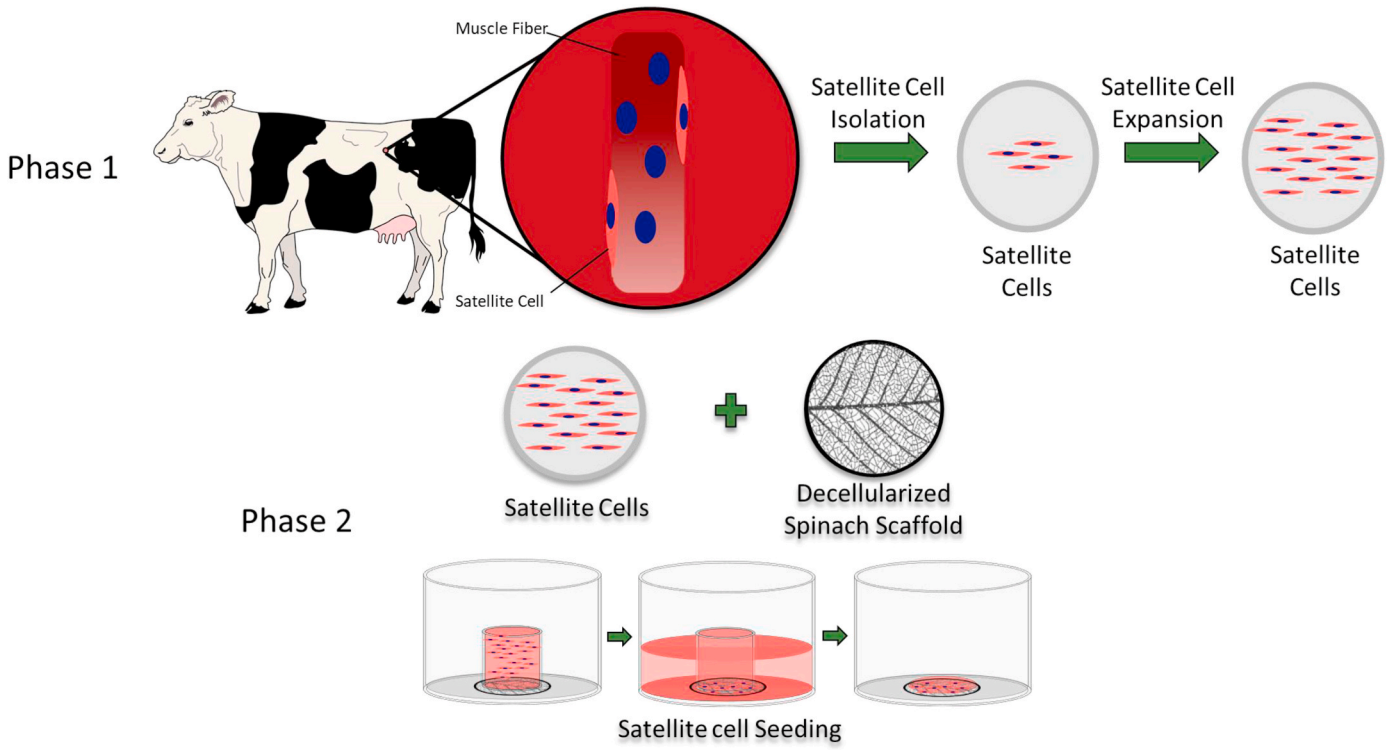

Fig. 1. | **Diagram of isolation and seeding of primary bovine satellite cells on decellularized spinach scaffold.** Tissue samples are acquired from 2 yr old Holstein bulls, then satellite cells are isolated and expanded. Cells are then cultured on decellularized spinach scaffolds and differentiated.

min to remove unwanted cells from the population prior to subculturing.

2.4. Seeding primary satellite cells

2.4.1. Decellularized spinach scaffold preparation

A 12 mm diameter circular punch was used to create scaffolds of uniform size. Scaffolds were then rehydrated using 10 mM tris buffer pH adjusted to 9.0 for 15 min at room temperature. Scaffolds were sterilized by incubating them in 70% ethanol for 30 min in a sterile dish inside of a laminar flow cabinet. After sterilization, scaffolds were rinsed three times with sterile PBS, waiting 5 min between rinses. Cell seeding was facilitated in a polydimethylsiloxane (PDMS) (Dow Chemical, Midland, MI, USA) coated polystyrene12-well plate (Thermo Fisher Scientific). The PDMS was formed by mixing the base elastomer and the curing agent at a ratio of 10:1 and degassed with a Bel-Art benchtop polycarbonate vacuum desiccator (Bel-Art Products, South Wayne, NJ, USA) for 1 hr to remove air bubbles. Approximately 1.5 ml of PDMS was poured into each well of the 12- well plate. The hydrophobic nature of the PDMS is used to prevent the cell suspension from spilling over onto the surface of the well. This also prevents cells from adhering to the surface of the plate. The hydrophobicity ensures that most of the cell suspension remains over the scaffold in the initial seeding period and that non-adhered cells can be washed away (Fig. 1). Sterile forceps were used to move each leaf scaffold to a well of the PDMS coated plate. Ten mm diameter (8 mm inner diameter) cloning wells (Corning Life Sciences, Tewksbury, MA, USA) were placed over the scaffolds to further confine the cell suspension to a specific area of the scaffold. The cloning wells remained in place for the duration of cell seeding.

2.4.2. Seeding cells on decellularized scaffolds

A 20 μl sample was removed from the cell suspension. A hemocytometer (Hausser Scientific, Horsham, PA, USA) was used to count the number of cells present in the sample and used to estimate the number of cells present in the total cell population. Approximately 200,000 cells were deposited directly onto the surface of the scaffold within the cloning well. After a 24 hr cell seeding period, cells that had not adhered were removed by gently rinsing the surface of the leaf with sterile PBS. The growth media inside of the cloning well was replaced, and an additional 1 ml of cell growth media was placed outside of the cloning well to entirely submerge the decellularized leaf (Fig. 1).

2.5. Viability assessment of seeded satellite cells

After seeding, cells were cultured in growth media. The growth media was replaced every 48 hr. The cells were studied at 7 and 14 days. At the end of each time point, the samples were stained using a LIVE/DEAD® staining kit (Thermo Fisher Scientific), a fluorescence-based viability stain composed of calcein AM and ethidium homodimer-1, and fixed in 4% paraformaldehyde for 10 min. Calcein AM is a fluorescent dye with an excitation wavelength of 494 nm and an emission wavelength of 517 nm used to label the body of live cells. Ethidium homodimer-1 is a fluorescent dye with an excitation wavelength of 517 nm and an emission wavelength of 617 nm used to label the nucleus of dead cells. Cells incubated in 70% ethanol for 30 min were used as a dead control. Samples were also stained with Hoechst 33342 (Thermo Fisher Scientific), a stain for DNA, used to confirm the presence of a cell nucleus. The viability percentage was calculated using the FIJI-ImageJ 1.8.0_172 (National Institutes of Health (NIH), Rockville, MD, USA) image processing program, downloaded from https://imagej.net/Fiji, to count dead cells and live cells present in each image (Kothari et al., 2009; Schindelin et al., 2012). A cell was considered dead if the ethidium homodimer-1 marker coincided with the nucleus of the cell. Cells lacking the dead marker were considered viable. The average of these images was used to represent the overall viability.

2.6. Assessment of differentiation potential

Cells were maintained in growth media for 2 days. The specimens were then changed to differentiation media containing only 2% heat-inactivated FBS with all other components unchanged. Differentiation

was measured at 5 and 12 days after exposure to the differentiation media (corresponding to 7 and 14 days after seeding). Specimens were fixed in 4% paraformaldehyde and stained for myosin heavy-chain (MyHC) using MF20 primary antibody (Developmental Studies Hybridoma Bank, Iowa City, IA, USA) and Alexa fluor 488 secondary antibody (Thermo Fisher Scientific). The specimen was stained with Hoechst 33342 to mark the presence of cell nuclei. Differentiation percentage was calculated using FIJI-ImageJ 1.8.0_172 software to count nuclei present in each image. A cell was determined to be differentiated if the nucleus coincided with the fluorescent signal of the secondary antibody of the MyHC antibody. All other nuclei were determined to be non-differentiated cells. The average of these images was used to represent the overall differentiation percentage for that sample.

2.7. Assessment of cell alignment

Alignment was measured at 5 and 12 days after exposure to the differentiation media. At the end of each time point, the specimens were fixed in 4% paraformaldehyde, and stained for F-actin using Phalloidin 488 (Life Technologies, Carlsbad, CA, USA) and Hoechst 33342.

Samples were imaged using a Leica SP5 point scanning confocal microscope (Leica Microsystems) at 40x. The alignment was determined by measuring the orientation of the cell nuclei and the cytoskeleton. The orientation of the nuclei was measured using the FIJI-ImageJ 1.8.0_172 image processing program by fitting an ellipse to each nucleus and measuring the angle of the maximum diameter relative to the horizontal axis of the image. The OrientationJ plug-in, downloaded from http://bigwww.epfl.ch/demo/orientation/, for FIJI-ImageJ 1.8.0_172 was used to measure the orientation of each microfilament in the image (Püspöki et al., 2016; Rezakhaniha et al., 2012). OrientationJ was also used to generate a color survey of each image to help visualize the orientation of each microfilament. The angle distribution of both the nuclei and the cytoskeleton were each obtained from this data. Relative alignment can be quantified by comparing the kurtosis, an index of the variability of the distribution of the measured variable, of each distribution to another. However, as directional data was being measured, directional statistics, mean vector angle and kappa, were used to study the distributions (Mardia, 1975).

The directional data from these images were imported into MATLAB (MathWorks, Natick, MA, USA) and processed using the CircStat toolbox (Berens, 2009). The circstat toolbox was used to calculate the mean vector length, angular standard deviation, and the kappa of the distribution. Kappa represents the concentration of angle values in the distribution (Dunn & Brown, 1986; Mardia, 1975), with a value that ranges from 0 to 1. A value of 0 indicates a distribution that lacks any discernable alignment, whereas a value of 1 indicates perfect and evident alignment. Alignment was measured for the cell nuclei and cytoskeletons independently. The average kappa value of each image was used to represent the overall alignment percentage of that sample.

3. Results

3.1. DNA quantification of decellularized leaf scaffolds

DNA quantification of the decellularized samples showed that decellularization removed most of the plant DNA from the leaf compared to non-decellularized leaf material of the same mass. Decellularized samples had an average DNA content of 73 ± 8 ng/mg. whereas non-decellularized leaf samples had an average DNA content of 720 ± 80 ng/mg.

3.2. Viability measurement of seeded satellite cells

After 7 days of incubation in growth media, the control group cultured on gelatin showed an average of 100% viability. This was also the case for all groups cultured on decellularized leaf scaffolds. After 14 days of incubation in growth media, the control group (Fig. 2a) maintained an average of 100% viability. Samples cultured on decellularized leaf scaffolds also showed strong evidence of overall cell viability (Fig. 2b). When compared to the control, all samples grown on the decellularized spinach scaffold showed comparable cell viability (Fig. 2c). A comparison using Welch's *t*-test suggested that there was no statistically significant difference in viability between cells grown on gelatin and the decellularized leaf scaffolds. Additionally, a one-way ANOVA test suggested that there was no significant difference in inter-animal viability among cells from all cows.

3.3. Measurement of differentiation potential

After 7 days of differentiation, 7.8 ± 1% of the control population grown on gelatin were positive for MyHC. Cells from all cows grown on decellularized spinach were positive for MyHC at 3.3 ± 1, 0.48 ± 0.48, and 0%, respectively, of the population. After 14 days of the differentiation protocol, a Welch's *t*-test used to compare cells grown on gelatin and decellularized leaf scaffolds suggested no significant differences (Fig. 3). In addition, one-way ANOVA testing suggested that there was no significant difference in differentiation among cells from Cows 1, 2, and 3 at both 7 and 14 days. However, a *t*-test between 7 and 14 days suggested statistical significance between timepoints and differentiation percentages, suggesting a significant increase in cell differentiation over time.

3.4. Measurement of cell alignment

Upon inspection of the color surveys produced using the orientation plugin, cells differentiated on gelatin for 7 days showed signs of alignment within the images, but no indications of alignment throughout the seeding region. The cell population from Cow 1 grown on the decellularized leaf scaffolds showed relative alignment across all technical replicates. However, these results were not shared with the other biological replicates. Cells grown on decellularized leaf scaffolds from Cows 2 and 3 qualitatively showed inconsistent alignment (Fig. 4a).

Similar to samples grown for 7 days, control cells differentiated for 14 days showed signs of local alignment within regions of the images, but no definitive alignment across the entire image. Cells from Cow 1 grown at 14 days on decellularized leaf scaffolds showed strong signs of alignment across entire images in all technical replicates. Cow 2 showed similar alignment in some images, but alignment was inconsistent between technical replicates. Cow 3, on the other hand, showed little signs of alignment between technical replicates.

Kappa values were used to quantitatively assess nuclear and cytoskeleton microfilament alignment within images of each sample. Samples differentiated for 7 days on gelatin had a relatively flat distributions with distinct peaks (Fig. 4b). Cells from Cow 1 that were cultured on the decellularized leaf scaffolds showed marginally better cytoskeleton alignment and significantly better nuclear alignment. Cytoskeletal and nuclear alignment for Cow 1 were 0.64 ± 0.05 and 0.37 ± 0.09, respectively. The average cytoskeleton and nuclear kappa values were 0.13 ± 0.2 and 0.15 ± 0.05 for Cow 2, and 0.17 ± 0.3 and 0.011 ± 0.2 for Cow 3. Cytoskeletal alignment for Cows 2 and 3 on leaf scaffolds were lower than that of their gelatin controls with cytoskeletal and nuclear kappa values of 0.45 ± 0.1 and 0.091 ± 0.1.

After 14 days of differentiation, cells grown on gelatin showed little change in alignment compared to 7 days. The average kappa values for cytoskeletal and nuclear alignment of the control group were measured as 0.39 ± 0.09 and 0.21 ± 0.13, respectively (Fig. 4c). Similarly, all samples grown on the decellularized leaf scaffolds for 14 days showed comparable alignment to that observed after 7 days. Cytoskeletal and nuclear alignment for Cow 1 grown for 14 days were measured as 0.71 ± 0.09 and 0.36 ± 0.01, respectively. The average cytoskeleton and nuclear kappa values were 0.47 ± 0.2 and 0.20 ± 0.03 for Cow 2 and 0.032 ± 0.087 and 0.05 ± 0.04 for Cow 3. Based on a Welch's *t*-test,

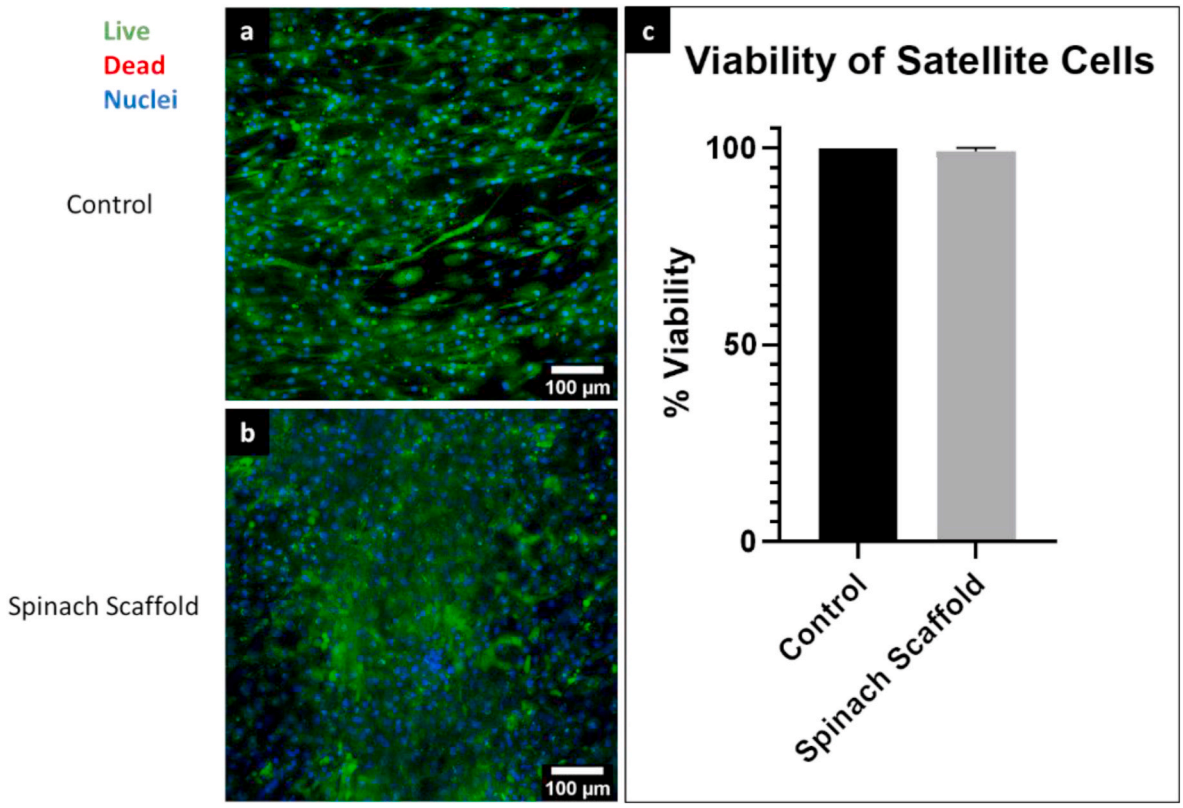

Fig. 2. | **Primary bovine satellite cells remain viable after being cultured on decellularized spinach scaffold for 14 days. a**) Live (green)/Dead (red) staining and Hoechst 33342 staining of nuclei (blue) of primary bovine satellite cells cultured on gelatin-coated glass (control) for 14 days. **b**) Live (green)/Dead (red) staining and Hoechst staining of nuclei (blue) of primary bovine satellite cells cultured on decellularized spinach scaffold for 14 days. **c)** Average cell viability of primary bovine satellite cells cultured on gelatin-coated glass (control) compared to decellularized spinach scaffold. (For interpretation of the references to color in this figure legend, the reader is referred to the Web version of this article.)

there was no statistically significant difference in local alignment between cells grown on gelatin and on decellularized leaf scaffolds for both cytoskeletal and nuclear alignment. A one-way ANOVA test suggested that there was no statistical significance in relative alignment among cells from Cows 1 and 2 at both time points. However, a comparison of Cows 1 and 3 suggested that there was a significant difference in relative alignment between the groups.

4. Discussion

The animal agriculture industry has long been a primary producer of food for Americans and many other countries. However, food production using conventional agriculture accounts for one of the highest contributors to environmental impact and resource usage both domestically and globally (EPA, 2019). When pondering ways to eliminate the detrimental effects that human activity has on the environment, reforming meat production methods should be considered. Cellular agriculture, the biomanufacturing of animal meat products, presents an alternative to conventional meat production.

The use of spinach as a substrate to grow bovine cells was studied. Previous studies have shown that various cell types can remain viable on decellularized plant scaffolds (Fontana et al., 2017; Gershlak et al., 2017). However, for production on a larger scale, a less time intensive method was developed. This method showed that decellularized spinach leaf samples had an average DNA content of 72 ± 8 ng/mg. Although this value falls short of the commonly accepted threshold of ≤50 ng/mg for sufficiently decellularized tissue (Crapo et al., 2011), it is not necessary to meet such a high standard for cultured meat application. The standard accepted DNA threshold was established to minimize adverse host reaction of xenogeneic DNA from implanted decellularized tissues. In this application, decellularized spinach leaves will be used for consumption, not implantation. Spinach is typically consumed whole, and its DNA has no known danger. Any adverse effects stemming from the presence of xenogeneic DNA will likely be observed in the viability assessment of cells seeded on the surface of this tissue.

Although previous studies have shown that various cell types can remain viable on decellularized plant scaffolds (Fontana et al., 2017; Gershlak et al., 2017), it was necessary to confirm that primary bovine satellite cells would survive for extended periods of time on spinach scaffolds. Results showed that all cells had an average viability of ≥98% after 14 days of culture. This shows that primary bovine satellite cells can remain viable on the surface of decellularized spinach scaffolds for extended periods of time with negligible cytotoxic effect.

Should the decellularization process need to be refined for commercial use in food processing, better results may be attained by increasing the concentration of detergents used and the duration of exposure. The decellularization process will also need to be optimized to ensure that all remnants of the detergents have been removed from the tissue. The US Food and Drug Administration (FDA) has established that bleach is safe for use in food products as long as the final concentration of available Cl is ‘200 ppm (FDA, 2013). Triton X-100 is not “Generally-Recognized-As-Safe” (GRAS). Polysorbate 60, a potential alternative to triton X-100, is approved by the FDA for direct addition to foods (FDA, 2021) In addition to being optimized to reduce the concentrations of remaining detergents in the leaf tissue after decellularization, the decellularization process may also need to be characterized and optimized to minimize adverse effects of the integrity of the surface, vascular network, and overall mechanical properties.

Previous studies have carried out preliminary characterization of decellularized plants including decellularized spinach (Fontana et al.,

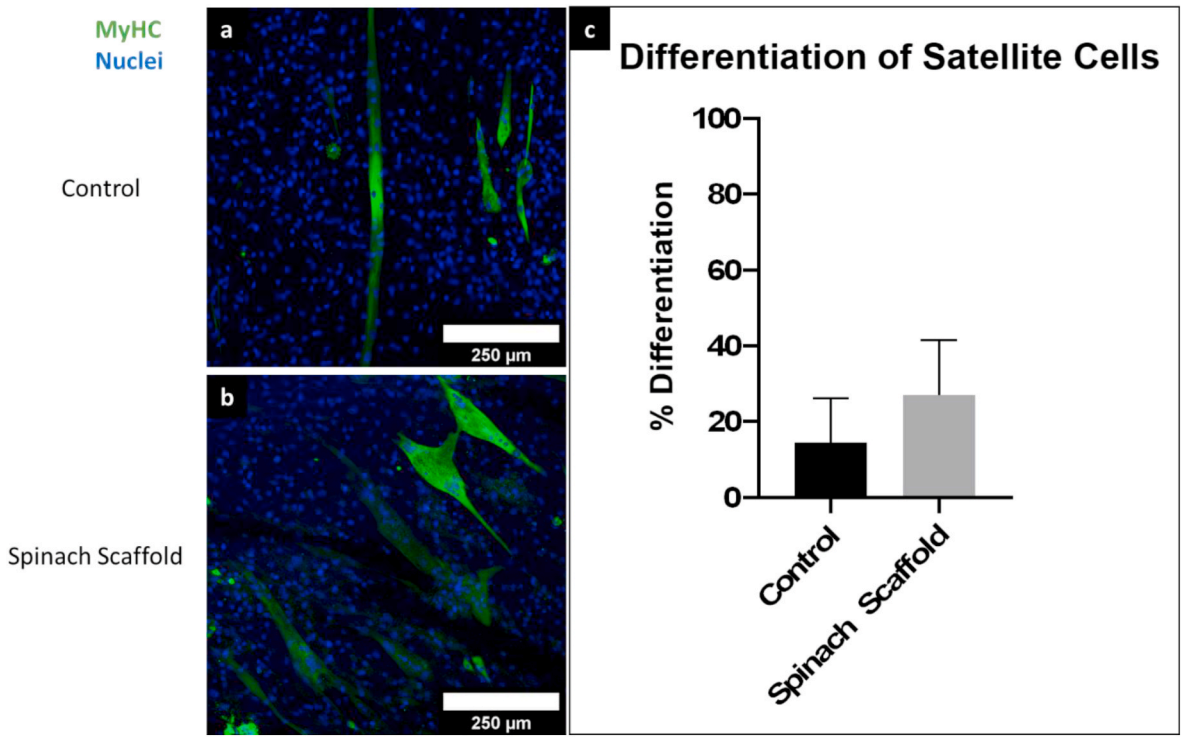

Fig. 3. | **Primary bovine satellite cells differentiate on decellularized spinach scaffold after 14 days. A)** MyHC staining (green) and Hoechst 33342 staining of nuclei (blue) of primary bovine satellite cells cultured on gelatin coated glass (control) for 14 days. **b)** Cells cultured on decellularized spinach scaffold for 14 days. **C)** Average percent differentiation of primary satellite cells cultured on gelatin coated glass (control) compared to decellularized spinach scaffold (N = 3 scaffolds, n = 3 biological replicates, p = 0.20). (For interpretation of the references to color in this figure legend, the reader is referred to the Web version of this article.)

2017; Gershlak et al., 2017). Scanning electron microscopy (SEM) has been used to characterize the surface of decellularized leaves (Fontana et al., 2017). This showed different topographical patterns and a highly porous structure, with pore sizes in decellularized plants ranging from <50 to ~300 μm (Fontana et al., 2017). Mechanical testing has shown that decellularized leaves have some similar mechanical properties to cardiac muscle. Decellularized spinach leaves were observed to have a maximum tangent modulus, a measure of elasticity, ranging from 0.2 – 0.5 MPa (Gershlak et al., 2017). Future studies may compare the mechanical properties of decellularized leaves to bovine skeletal muscle and other muscle tissues that comprise other meat products. These properties may influence the differentiation and alignment of cells cultured on the surface (Engler et al., 2004). The mechanical properties may also contribute to the overall texture of meat grown on decellularized plants. This study has also shown that muscle tissue could be formed on decellularized spinach from primary bovine satellite cells. At 7 days post-seeding, the differentiation efficiency was significantly higher among the control group when compared to the cells cultured on decellularized spinach scaffolds. However, at 14 days post-seeding, differentiation efficiency improved on decellularized spinach. The cause of the low differentiation efficiency on the scaffolds at 7 days is not known, but delayed differentiation could potentially suggest an increase in myoblast proliferation and self-renewal (Riederer et al., 2012). This can be explored in the future using flow cytometry to quantify the population of cells that are expressing PAX7 and Ki67 over time.

While these results showed that primary bovine satellite cells can differentiate on the surface of decellularized spinach, for commercial use it will be necessary to optimize the differentiation conditions to increase the number of differentiated cells in the tissue. Such refinement may include further purification of the satellite cells population with the use of cell sorting tools such as fluorescence activated cell sorting (FACS) and magnetic activated cell sorting (Eberli et al., 2009) to isolate $PAX7^{+}$ cells. Vascular cell adhesion molecules have been shown to be a useful surface marker for achieving pure populations of $PAX7^{+}$ satellite cells using FACS (Riaz et al., 2016). Differentiation efficiency may also be improved by modifying the media formulation of satellite cells grown on tissue culture plastic. Such changes may include elimination of growth factors and significant reduction or elimination of animal derived serum. Further studies can be done to assess the maturity and function of differentiated cells by staining for additional markers such as desmin and sarcomeric α-actinin. In addition to the composition of the tissue, the arrangement of cells within the tissue is important. To replicate the structure of muscle tissue *in vivo*, cells must be aligned with one another to form muscle fibers.

Measurements of cellular alignment suggested that primary satellite cells do not spontaneously align on the surface of the scaffold. However, on many samples there were examples of high alignment across entire regions. It is possible that the local surface topography may have had some influence on how cells arranged themselves. Fontana et al. (2017) showed various surface topography in different plant species, which varied depending on location within the leaf. They also showed that cells aligned to topographical cues, suggesting that these features may be able to direct cell alignment and differentiation. For example, regions of the leaf that coincide with large vasculature channels have crevasses directly above them. Cells that are seeded onto the leaf in these regions will settle into these crevasses. It is possible that local alignment is encouraged along the axis of the channel. Whereas regions that do not coincide with a vascular channel may lack these topographical cues. To assess the impact that surface topography may have on alignment, future studies can compare local alignment of cells grown on various regions of the leaf as this may be advantageous to create organized muscle structures. Additionally, alternative plant leaves with grooved topographical features can be explored.

Another important factor in cell alignment could be the specific animal source used to acquire primary cells. To minimize biological variation, muscle samples were taken from the same region of cows of similar age, same sex, and same breed. However, there is still the possibility that the animals may have been raised in separate herds. This

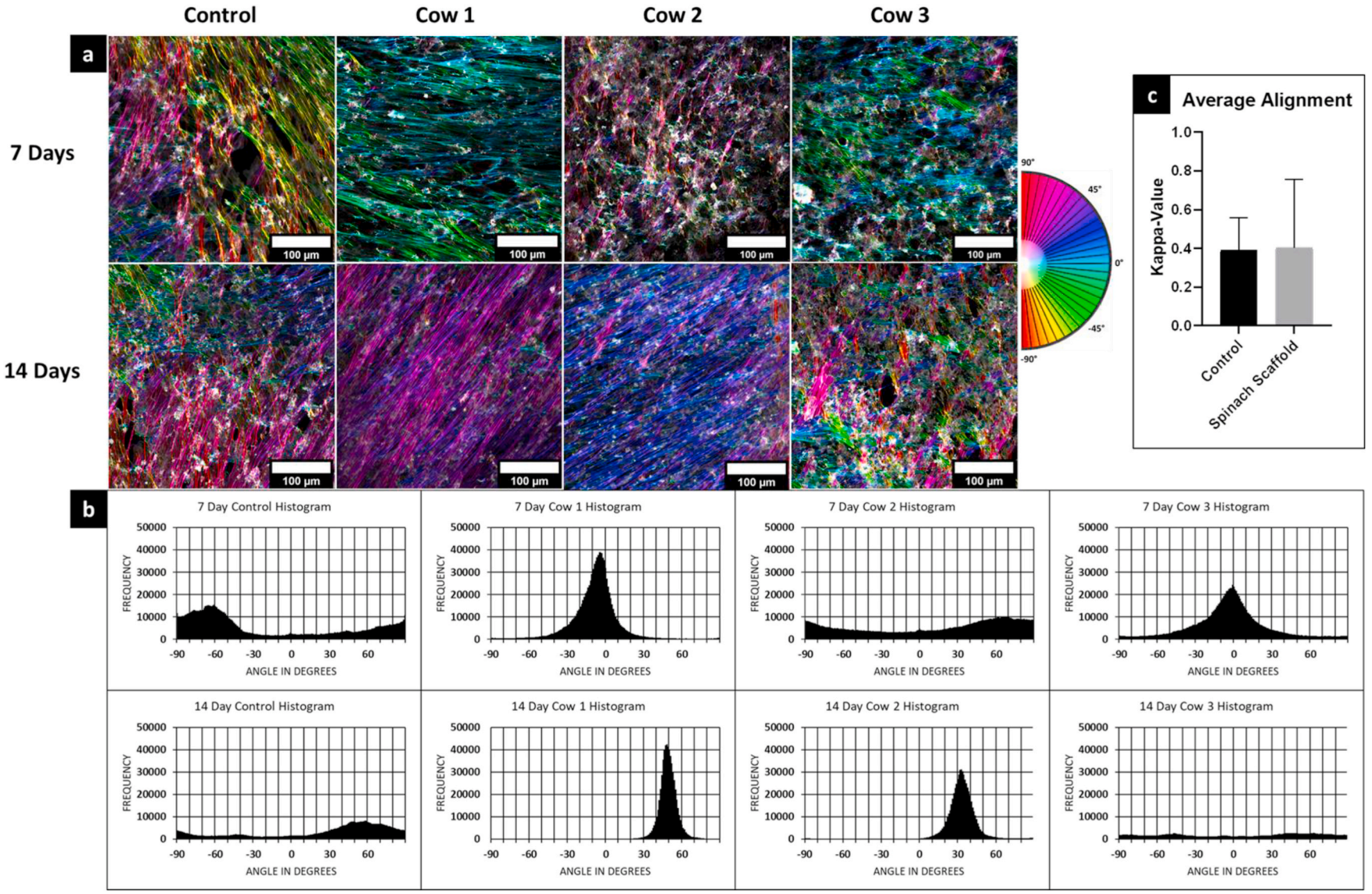

Fig. 4. | **Alignment was showed on several samples but remains inconsistent between samples. a)** Directional analysis color survey indicates the direction of primary bovine satellite cell cytoskeletal (microfilament) cultured on gelatin coated glass (control) and decellularized spinach scaffold at 7 and 14 days. Each color represents a different alignment angle. **b)** Cytoskeleton microfilament orientation histograms of primary bovine satellite cells cultured on gelatin coated glass (control) and decellularized spinach scaffold for 7 and 14 days. **c)** Average cytoskeleton microfilament alignment of primary satellite cells cultured on gelatin coated glass (control) vs. decellularized spinach scaffold (N = 3 scaffolds, n = 3 biological replicates, p = 0.30). (For interpretation of the references to color in this figure legend, the reader is referred to the Web version of this article.)

may have contributed to the significant variation observed in alignment. cells isolated from one cow consistently showed cellular alignment, whereas one cow consistently showed minimal alignment. Potential sources of variation should be investigated to optimize cell alignment by sourcing tissues from different cow herds with different environmental factors.

This study has shown the potential use of decellularized spinach leaves for the development of laboratory-grown meat. There is still significant work needed before this technology can be used commercially. One of the challenges is acquiring a sufficiently large and homogeneous satellite cell population (Zhang et al., 2020). This will require immense bioreactor systems to facilitate satellite cell proliferation and differentiation (Zhang et al., 2020). Satellite cell are anchorage-dependent, meaning such bioreactors would need to incorporate microcarriers or some form of substrate for the cells to adhere to (Verbruggen et al., 2018). Lastly, the shear stresses within the bioreactor also need to be optimized to prevent cell death. In addition to longer term cell growth studies, the nutritional content of this biomanufactured cell-based meat needs to be quantified. Additional cell types, for example adipose cells, should also be included in the final product. Samples of meat with a thickness larger than 200 μm may be obtained from stacking cell-seeded leaves, however, the diffusion of nutrients into the meat (and the removal of metabolites) must still be characterized.

5. Conclusions

Nature has solved the problem of oxygen diffusion by developing complex vascular networks to bring oxygen deep within the tissue. Decellularization exploits this for numerous tissue engineering applications (Guyette et al., 2016). The appeal of using decellularized spinach for meat developments lies not only in its natural vascular network, but also in its edibility and commonality. Using non-edible synthetic materials requires further processing to thoroughly remove the scaffold from the cultured tissue before consumption. An edible material would eliminate the need to separate the scaffold from the tissue as they will both be consumed (Enrione et al., 2017). Furthermore, spinach is cheap, accessible, and well-known to consumers. These qualities are important for commercialization and will simplify the process of scaling up production.

CRediT authorship contribution statement

Jordan D. Jones: Conceptualization, Methodology, Software, Formal analysis, Data curation, Investigation, Resources, Visualization, Funding acquisition, Writing – original draft, Writing – review & editing. **Alex S. Rebello:** Investigation, Writing – review & editing. **Glenn R. Gaudette:** Conceptualization, Supervision, Validation, Funding acquisition, Writing – review & editing.

Declaration of competing interest

The authors declare the following financial interests/personal relationships which may be considered as potential competing interests: A patent application has been filed for the decellularized spinach scaffold and its use for cultured meat production.

Acknowledgments

This work is supported through a research fellowship provided by New Harvest, USA (to JDJ). The authors would like to thank Dr. David Kaplan for supplying primary satellite cells used for preliminary data collection. Preliminary work for this study was done by Emily Robbins, Alex Rebello, Brian Moore, Daniel Sochacki, and Fatin Alkhaledi. The authors would also like to thank Elina Saint-Elme, Rebecca Lee, Lily Cordner, and Kirsten Stevens for assisting in manuscript preparation.

References

Aiking, H. (2011). Future protein supply. *Trends in Food Science & Technology, 22*(2–3), 112–120. https://doi.org/10.1016/j.tifs.2010.04.005

Berens, P. (2009). CircStat : A MATLAB toolbox for circular statistics. *Journal of Statistical Software, 31*(10), 1–21. https://doi.org/10.18637/jss.v031.i10

Burton, N. M., Vierck, J. L., Krabbenhoft, L., Byrne, K., & Dodson, M. V. (2000). Methods for animal satellite cell culture under a variety of conditions. *Methods in Cell Science, 22*(1), 51–61. https://doi.org/10.1023/A:1009830114804

Crapo, P. M., Gilbert, T. W., & Badylak, S. F. (2011). An overview of tissue and whole organ decellularization processes. *Biomaterials, 32*(12), 3233–3243. https://doi.org/10.1016/j.biomaterials.2011.01.057

Datar, I., & Betti, M. (2010). Possibilities for an *in vitro* meat production system. *Innovative Food Science & Emerging Technologies, 11*(1), 13–22. https://doi.org/10.1016/j.ifset.2009.10.007

Dunn, G. A., & Brown, A. F. (1986). Alignment of fibroblast on grooved substrate described by a simple geometric transformation. *Journal of Cell Science, 340*, 313–340.

Eberli, D., Soker, S., Atala, A., & Yoo, J. J. (2009). Optimization of human skeletal muscle precursor cell culture and myofiber formation in vitro. *Methods, 47*(2), 98–103. https://doi.org/10.1016/j.ymeth.2008.10.016

Ellis, E. C., Goldewijk, K. K., Siebert, S., Lightman, D., & Ramankutty, N. (2010). Anthropogenic transformation of the biomes, 1700 to 2000. *Global Ecology and Biogeography, 19*(5), 589–606. https://doi.org/10.1111/j.1466-8238.2010.00540.x

Engler, A. J., Griffin, M. A., Sen, S., Bönnemann, C. G., Sweeney, H. L., & Discher, D. E. (2004). Myotubes differentiate optimally on substrates with tissue-like stiffness: Pathological implications for soft or stiff microenvironments. *Journal of Cell Biology, 166*(6), 877–887. https://doi.org/10.1083/jcb.200405004

Enrione, J., Blaker, J. J., Brown, D. I., Weinstein-Oppenheimer, C. R., Pepczynska, M., Olguín, Y., Sánchez, E., & Acevedo, C. A. (2017). Edible scaffolds based on non-mammalian biopolymers for myoblast growth. *Materials, 10*(12), 1–15. https://doi.org/10.3390/ma10121404

EPA. (2019). Sources of greenhouse gas emissions. In *Climate change* (pp. 1–2). Washington, DC, USA: Environmental Protection Agency. https://www.epa.gov/ghgemissions/sources-greenhouse-gas-emissions%0Ahttp://www.epa.gov/climatechange/ghgemissions/sources/transportation.html.

FDA. (2013). Food additive status list: Morpholina. In *U.S. Food and Drug administration (issue 240)*. Rockville, MD, USA: FDA. https://www.fda.gov/food/ingredientspackaginglabeling/foodadditivesingredients/ucm091048.htm%0Ahttps://www.fda.gov/Food/IngredientsPackagingLabeling/FoodAdditivesIngredients/ucm091048.htm#ftnO%0Ahttp://www.fda.gov/Food/IngredientsPackagingLabeling/FoodAdd.

FDA. (2021). *Code of federal regulations title 21* (pp. 3–6). Rockville, MD, USA: Government Printing Office.

Fontana, G., Gershlak, J., Adamski, M., Lee, J. S., Matsumoto, S., Le, H. D., Binder, B., Wirth, J., Gaudette, G., & Murphy, W. L. (2017). Biofunctionalized plants as diverse biomaterials for human cell culture. *Advanced Healthcare Materials, 6*(8), 1–9. https://doi.org/10.1002/adhm.201601225

Gershlak, J. R., Hernandez, S., Fontana, G., Perreault, L. R., Hansen, K. J., Larson, S. A., Binder, B. Y. K., Dolivo, D. M., Yang, T., Dominko, T., Rolle, M. W., Weathers, P. J., Medina-Bolivar, F., Cramer, C. L., Murphy, W. L., & Gaudette, G. R. (2017). Crossing kingdoms: Using decellularized plants as perfusable tissue engineering scaffolds. *Biomaterials, 125*, 13–22. https://doi.org/10.1016/j.biomaterials.2017.02.011

Guyette, J. P., Charest, J. M., Mills, R. W., Jank, B. J., Moser, P. T., Gilpin, S. E., Gershlak, J. R., Okamoto, T., Gonzalez, G., Milan, D. J., Gaudette, G. R., & Ott, H. C. (2016). Bioengineering human myocardium on native extracellular matrix. *Circulation Research, 118*(1), 56–72. https://doi.org/10.1161/CIRCRESAHA.115.306874

Hasan, A. F., Laurent, F., Messner, F., Bourgoin, C., & Blanc, L. (2019). Cumulative disturbances to assess forest degradation using spectral unmixing in the northeastern Amazon. *Applied Vegetation Science, 22*(3), 394–408. https://doi.org/10.1111/avsc.12441

Kothari, S., Chaudry, Q., & Wang, M. D. (2009). Automated cell counting and cluster segmentation using concavity detection and ellipse fitting techniques. In *, Vol. 2. Proceedings - 2009 IEEE international symposium on biomedical imaging: From nano to macro* (pp. 795–798). Boston, MA, USA: ISBI 2009. https://doi.org/10.1109/ISBI.2009.5193169.

Mardia, K. V. (1975). Statistics of directional data. *Journal of the Royal Statistical Society, 37*(3), 349–393.

Novosel, E. C., Kleinhans, C., & Kluger, P. J. (2011). Vascularization is the key challenge in tissue engineering. *Advanced Drug Delivery Reviews, 63*(4), 300–311. https://doi.org/10.1016/j.addr.2011.03.004

Püspöki, Z., Storath, M., Sage, D., & Unser, M. (2016). Transforms and operators for directional bioimage analysis: A survey. *Advances in Anatomy, Embryology, and Cell Biology, 219*, 69–93. https://doi.org/10.1007/978-3-319-28549-8_3

Ray, D. K., Mueller, N. D., West, P. C., & Foley, J. A. (2013). Yield trends are insufficient to double global crop production by 2050. *PloS One, 8*(6). https://doi.org/10.1371/journal.pone.0066428

Rezakhaniha, R., Agianniotis, A., Schrauwen, J. T. C., Griffa, A., Sage, D., Bouten, C. V. C., Van De Vosse, F. N., Unser, M., & Stergiopulos, N. (2012). Experimental investigation of collagen waviness and orientation in the arterial adventitia using confocal laser scanning microscopy. *Biomechanics and Modeling in Mechanobiology, 11*(3–4), 461–473. https://doi.org/10.1007/s10237-011-0325-z

Riaz, N., Wolden, S. L., Gelblum, D. Y., & Eric, J. (2016). Isolation of skeletal muscle stem cells by fluorescence-activated cell sorting. *Nature Protocols, 118*(24), 6072–6078. https://doi.org/10.1002/cncr.27633.Percutaneous

Riederer, I., Negroni, E., Bencze, M., Wolff, A., Aamiri, A., Di Santo, J. P., Silva-Barbosa, S. D., Butler-Browne, G., Savino, W., & Mouly, V. (2012). Slowing down differentiation of engrafted human myoblasts into immunodeficient mice correlates with increased proliferation and migration. *Molecular Therapy, 20*(1), 146–154. https://doi.org/10.1038/mt.2011.193

Schindelin, J., Arganda-Carreras, I., Frise, E., Kaynig, V., Longair, M., Pietzsch, T., Preibisch, S., Rueden, C., Saalfeld, S., Schmid, B., Tinevez, J. Y., White, D. J., Hartenstein, V., Eliceiri, K., Tomancak, P., & Cardona, A. (2012). Fiji: An open-source platform for biological-image analysis. *Nature Methods, 9*(7), 676–682. https://doi.org/10.1038/nmeth.2019

Shapiro, P. (2018). *Clean meat: How growing meat without animals will revolutionize dinner and the world.* New York, NY, USA: Simon and Schuster.

Verbruggen, S., Luining, D., van Essen, A., & Post, M. J. (2018). Bovine myoblast cell production in a microcarriers-based system. *Cytotechnology, 70*(2), 503–512. https://doi.org/10.1007/s10616-017-0101-8

Zhang, G., Zhao, X., Li, X., Du, G., Zhou, J., & Chen, J. (2020). Challenges and possibilities for bio-manufacturing cultured meat. *Trends in Food Science & Technology, 97*(September 2019), 443–450. https://doi.org/10.1016/j.tifs.2020.01.026